Design and Synthesis of Ultrasensitive Off-On Fluoride Detecting Fluorescence Probe via Autoinductive Signal Amplification

Jiun-An Gu[1], Veerappan Mani[1], Sheng-Tung Huang[1,2*]

[1]Department of Chemical Engineering and Biotechnology, National Taipei University of Technology, Taipei, Taiwan (Republic of China).

[2]Graduate Institute of Biomedical and Biochemical Engineering, National Taipei University of Technology, Taipei, Taiwan (Republic of China).

* Corresponding author: Email id: ws75624@ntut.edu.tw Tel.: +886 2271-2171 2525; Fax: +886-02-2731-7117.

Abstract

We prepared an off–on fluorometric probe, DPF_1, by incorporating the concept of autoinductive signal amplification into its molecular design. In the presence of fluoride, DPF_1 undergoes a cascade of self-immolative reactions concomitant with unmasking fluorogenic coumarin which resulting in the ejection of two fluoride ions. These fluoride ions are continuously activates the cascade reaction and accumulating coumarins which leading to the exponentially amplifying the signal with high sensitivity. The fluorescence signal generated by this cascade reaction is rapid, specific and insensitive to other anions. Its limit of detection was 0.5 pM, much lower than other current methods of fluoride detection. In addition, DCC, a long wavelength fluorometric probe was prepared. Interestingly, an assay platform coupling DPF_1 and DCC showed outstanding sensing ability at higher wavelengths, suggesting that this method can be promising method for the sensitive and selective detection of fluoride in biological samples. The practical applicability of the proposed approach has been demonstrated in urine and water samples.

Keywords: Autoinductive signal amplification, Coumarins, Fluorescence spectroscopy, Fluorescent probes, Fluoride

1. Introduction

Most currently utilized techniques capable of assaying analytes with high sensitivity and selectivity [1], including enzyme-linked immunosorbent assays (ELISA) [2], polymerase chain reaction (PCR) [3], and bio-barcode assays [4] are relying on antibodies, enzymes and biomolecules [5]. The unique chemical structures of these biomolecules serve as recognition sites to distinguish the analyte from similar molecules, enhancing the specificity of these assays. Moreover, the concept of continuous signal revealing reactions triggered by analyte–probe recognition embedded within these methods amplifies the signal for high sensitivity. In most cases, however, the reagents used in these assays are either thermally unstable or are not stable for prolonged periods of time. Thus, practical difficulties are encountered when trying to use these reagents in analyses at ambient temperature. To circumvent this limitation and to achieve high sensitivity and specificity, new approaches have been used to design auto-inductive small molecular probes that mimic these biomolecules (scheme 1a) [6-12]. These auto-inductive molecular probes are equipped with unique triggering groups which are selectively interacting with the analyte of interest via designated chemical reactions pathway. These reactions trigger a cascade of self-immolative reactions, which simultaneously unmask the signal molecules (chromogenic or fluorogenic) and spontaneously liberate the signal transduction molecules [12]. The latent generated signal transduction molecules continuously induce the auto-inducible molecular probes to undergo self-immolative signal revealing reactions, resulting in the accumulation of signal molecules. Thus, this cyclic reaction process results in the signal amplification required for high sensitivity [13].

Fluoride ion chemosensors are in high demand due to the importance of fluoride in a variety of healthcare and environmental contexts [14-17]. The US Environmental Protection Agency (EPA) has recommended an allowed upper limit of 2 ppm fluoride in water [18]. Nevertheless, the detection of low concentrations of fluoride in polar and aqueous solutions remains challenging without expensive analytical equipment. Several chromogenic and fluorogenic probes, which rely on hydrogen bonds or Lewis acid coordination, have been used to detect low fluoride concentrations [19, 20]. Most of these probes can only be utilized in organic solvents to detect tetrabutylammonium (TBA^+) fluoride, however cannot be used to detect inorganic fluoride salts [21-23]. Other fluoride sensors based on the chemical affinity between fluoride and silicon have been used to detect inorganic fluoride salts in polar solvents; however, the sensitivity of these sensors can be influenced by increasing the water concentration in the detection system [24-28].

Designing latent self-immolative ratiometric chemical probes and exploring their applications are ongoing research interests of our research group [29-32]. We recently used a quinone-methide-type of rearrangement reaction to successfully design an off–on colorimetric probe which detects fluoride; however, the limit of detection (LOD) of this probe was judged unsatisfactory by the EPA [18]. To improve the LOD and sensitivity of this probe, we sought to expand its signal-revealing mechanism by incorporating an exponential signal amplification approach. Using this method, we have designed a new auto-inductive off–on fluorogenic probe, DPF_1, as a ratiometric sensor for the ultrasensitive detection of inorganic fluoride [scheme 1a]. The chemical structure of the DPF_1 and schematic illustration of its autoinductive signal-revealing amplification mechanism induced by fluoride are briefly outlined in Scheme 1b. The DPF_1 probe is composed of 4-(tert-butyldiphenylsilyloxy) trigger group attached to the latent reporter coumarin, which carries two fluoride moieties as signal amplifiers (Scheme 1a). Fluoride ions are induced the removal of a silyl protecting trigger group on DPF_1 which resulting in a cascade of self-immolative reactions through a quinone-methide type of rearrangement reaction to generate a fluorogenic reporter, coumarin (b), along with the ejection of two additional fluorides. The latent generated fluorides then continuously induce self-immolative reactions of the unreacted DPF_1. This cyclic reaction process is leading to the accumulation of fluorogenic coumarins and resulting in signal amplification. The fluorogenic probe, DPF_1, is achieved very low LOD of 0.5 pM, lower than any other current known method used in the determination of fluoride [14-17, 33]. To our knowledge, the lowest LOD for the detection of inorganic fluoride with currently known methods are in the low nanomolar ranges. Few recent studies have reported closely related examples of signal amplification for the detection of fluoride, however, they are using colorimetric and absorption detection methods and LOD of their probes were in the low nanomolar range [13, 34]. In contrast, our fluorescence probe method can detect fluoride in the upper picomolar range with LOD of 0.5 pM which surpasses the LODs of existing methods. The conceptual idea of Baker et al., and Perry-Feigenbaum et al. furnished us an exciting impression to design a unique fluorescence probe to enhance the signal and push the LOD from nanomolar to picomolar level by employing fluorescence spectroscopy. In addition, an assay platform coupling DPF_1 and DCC (a long wavelength fluorometric probe) showed outstanding sensing ability at higher wavelengths, suggesting that this method could be a promising method for the selective detection of fluoride in biological samples. Both DPF_1 and DCC are highly stable for prolonged periods when stored above 0°C, while their syntheses involve simple and straightforward procedures.

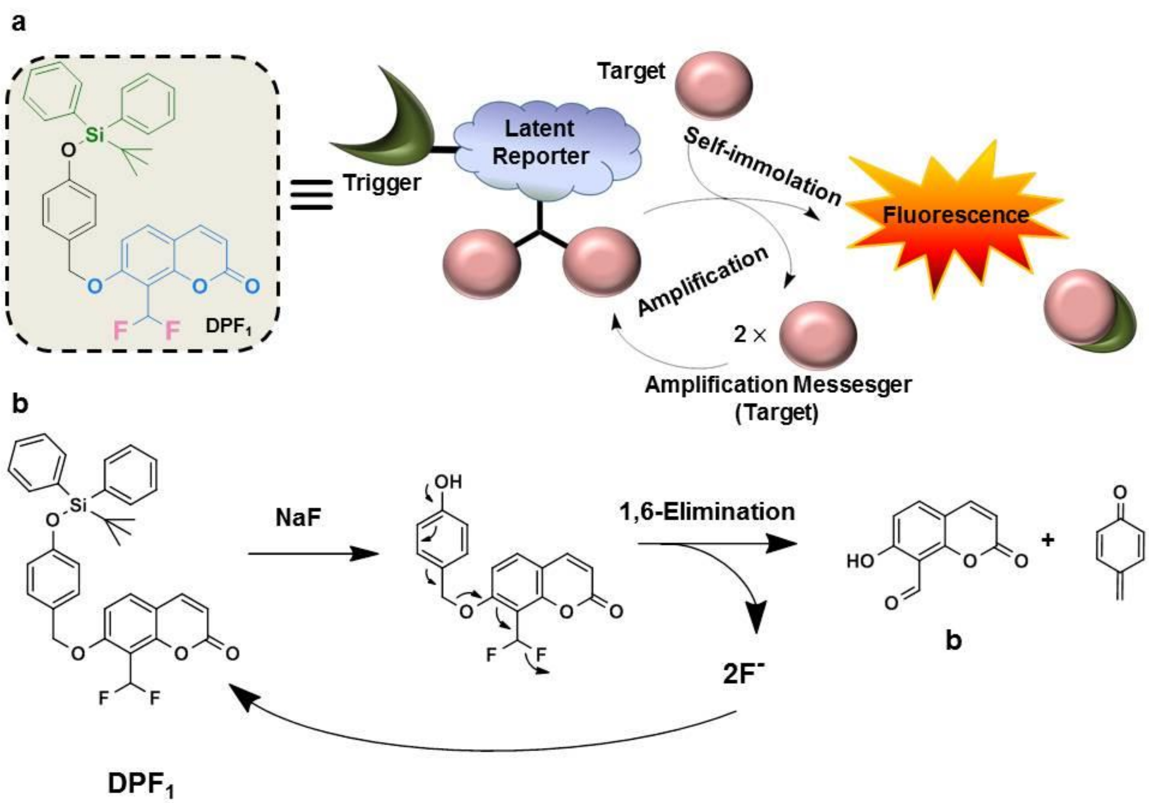

Scheme 1. Pathway by which DPF_1 detects fluoride and releases two equivalents of fluoride to propagate the auto-inductive signal amplification process

2. Experimental section

2.1. Synthesis of 7-((4-(tert-butyldiphenylsilyloxy)benzyl)oxy)-8-formylcoumarin (DPA_1)

A solution of 4-(tert-butyldiphenylsilyloxy)benzyl chloride (a) (1 g, 2.62 mmol), 7-hydroxy-8-formylcoumarin (0.4 g, 2.1 mmol), KI (0.87 g, 5.24 mmol) and K_2CO_3 (2.9 g, 21 mmol) in dry DMF (20 mL) are stirred overnight at room temperature under argon atmosphere (Scheme S1 [29, 33]. The resulting mixture was diluted with water (150 mL). The organic layer was extracted with ethylacetate (EtOAc, 3×150 mL), dried with $MgSO_4$ and concentrated in vacuo and then purified by column chromatography on silica gel (MeOH/toluene=1/9) yielding the title compound (54%, 0.609 g) as a milky solid. ^{1}H NMR (300 MHz, $CDCl_3$, ppm): δ=1.08 (s, 9H), 5.11 (s, 2H), 6.29 (d, 1H, J=9.6), 6.76 (dd, 2H, J = 6.45, J=1.95 Hz), 6.92 (d, 1H, J=9 Hz), 7.16 (d, J=8.7 Hz), 7.32-7.41 (m, 6H), 7.54 (d, 1H, J=9 Hz), 7.60 (d, 1H, J=9.6 Hz), 7.67-7.70 (m, 4H), 10.61 (s, 1H) (Fig. S1). ^{13}C NMR (75 MHz, $CDCl_3$, ppm): δ=19.47, 26.48, 71.14, 109.60, 112.69, 113.15, 114.13, 120.01, 127.52, 127.84, 128.45, 130.00, 132.63, 133.95, 135.50, 143.01, 155.65, 155.79, 159.55, 162.59, 186.89 (Fig. S2). MS (ESI+): Calcd for [$C_{33}H_{30}O_5Si$ + Na] = 557.17, found = 557.1; Calcd for [$C_{33}H_{30}O_5Si$ + K] = 573.14, found = 573.1 (Fig. S3). HRMS (TOF MS AP+): calcd for [$C_{33}H_{30}O_5Si$ +] = 534.1863, found = 534.1862.

2.2. Synthesis of 7-((4-(tert-butyldiphenylsilyloxy)benzyl)oxy)-8-(difluoromethyl)-coumarin (DPF$_1$)

DPA$_1$ (0.4 g, 0.75 mmol) solution was dissolved in dichloromethane (DCM, 15 mL) and cooled to – 20°C. *N*,*N*-Diethylaminosulfur trifluoride (DAST, 0.36 g, 2.25 mmol) was added to DPA$_1$ and the reaction mixture was warmed to – 5°C (Scheme S1). The reaction mixture was stirred under these conditions for 6 h, while the reaction progress was monitored by TLC (methanol (MeOH)/toluene = 1:9). Upon completion of the reaction, the reaction mixture was cooled to – 78°C and quenched with 5 drops of water. The resulting residue was dried with $MgSO_4$ and concentrated in vacuo, then purified by column chromatography on silica gel (MeOH/toluene=3/97) yielding the title compound (31%, 0.13 g) as a milk yellow solid. ^{1}H NMR (300 MHz, $(CD_3)_2CO$, ppm): δ=1.09 (s, 9H), 5.22 (s, 2H), 6.29 (d, 1H, J=9.6 Hz), 6.82 (d, 2H, J=8.4 Hz), 7.21 (d, 1H, J=8.7 Hz), 7.26 (t, 1H, J=45.3 Hz), 7.29 (d, 2H, J=8.4 Hz), 7.39–7.50 (m, 6H), 7.73-7.79 (m, 5H), 7.93 (d, 1H, J=9.6 Hz) (Fig. S4). ^{13}C NMR (75 MHz, $CDCl_3$, ppm): δ =19.83, 26.74, 71.46, 109.84, 110.14, 110.49, 113.94, 114.32, 120.48, 128.74, 129.69, 129.87, 130.97, 133.04, 133.30, 136.20, 144.48, 154.37, 156.40, 159.63, 160.64 (Fig. S5). MS (ESI+): Calcd for [$C_{33}H_{30}$ F_2O_4Si + Na] = 579.17, found=579.2 (Fig. S6). HRMS (TOF MS AP+): calcd for [$C_{33}H_{30}$ F_2O_4Si +] = 556.1881, found = 556.1882.

2.3. Synthesis of 3-(benzothiazol-2-yl)-4-carbonitrile-7-((4-(tert-butyldiphenylsilyl oxy)benzyl)oxy)coumarin (DCC)

A solution of 4-(tert-butyldiphenylsilyloxy)benzyl chloride (a) (0.7 g, 1.84 mmol), 3-(2'-benzothiazolyl)-4-carbonitrile-7-hydroxycoumarin (c) (0.88 g, 2.76 mmol), KI (0.92 g, 5.52 mmol) and K_2CO_3 (2.54 g, 18.4 mmol) in dry DMF (15mL) was stirred overnight at room temperature under argon atmosphere (Scheme S2) [32]. The resulting mixture was diluted with water (150 mL). The organic layer was extracted with EtOAc (3 × 150 mL), dried with $MgSO_4$ and concentrated in vacuo, then purified by column chromatography on silica gel (EtOAc/toluene = 0.5/9.5) yielding the title compound (67%, 1.22 g) as an orange solid. ^{1}H NMR (300 MHz, $CDCl_3$, ppm): δ=1.083 (s, 9H), 5.03 (s, 2H), 6.78 (d, 1H, J=8.4 Hz), 6.93 (d, 2H, J=2.4 Hz), 7.07 (dd, 1H, J=9, J=2.4 Hz), 7.15 (d, 2H, J=84 Hz), 7.325-7.554 (m, 8H), 7.697 (dd, 4H, J=7.8, J=1.5 Hz), 7.97–8.02 (m, 2H), 8.214 (d, 1H, J=8.1 Hz) (Fig. S7). ^{13}C NMR (75MHz, $CDCl_3$, ppm): δ=19.42, 26.43, 70.89, 101.76, 110.97, 113.57, 115.32, 120.03, 120.68, 121.46, 122.15, 124.12, 126.45, 126.77, 127.25, 127.81, 128.89, 129.12, 129.98, 132.56, 135.46, 137.24, 152.16, 154.42, 156.01, 156.63, 158.81, 164.02 (Fig. S8). MS (ESI+): Calcd for $[C_{40}H_{32}N_2O_4SSi +]$: 664.19, found 664.2 (Fig. S9). HRMS (TOF MS AP+): calcd for $[C_{40}H_{32}N_2O_4SSi +]$: = 664.1852, found = 664.1852.

2.4. Assay conditions for the detection of fluoride using DPF_1

A stock solution of DPF_1 was prepared in acetonitrile, while stock solutions of all other reagents were prepared in water. In a typical assay, DPF_1 (50 µM) was incubated in an acetonitrile:pyridine:water (94:1:5 [v/v/v]; APW) solution at respective temperature and time. The assay conditions such as ratio between the solvents, temperature and time were optimized to get maximum fluorescence response for the detection of fluoride. Various amounts of NaF or other anions (in the case of selectivity studies) were added, and the release of 7-hydroxy-8-formylcoumarin (b) was monitored by recording fluorescence spectra at λ_{ex} = 360 nm and λ_{em} = 445 nm.

2.5. Assay conditions for the detection of fluoride using two probes approach (DPF_1 and DCC)

Stock solutions of both DPF_1 and DCC were prepared in acetonitrile, while stock solutions of all the other reagents were prepared in water. In a typical assay, DPF_1 (50 µM) and DCC (5 µM) were incubated in APW solution at corresponding temperature and time. Various amounts of NaF or other anions were added, and the release of 3-(2'-benzothiazolyl)-4-

carbonitrile-7-hydroxycoumarin (c) was monitored by recording fluorescence spectra at λ_{ex}=500 nm and λ_{em}=595 nm.

3. Results and discussion

DPF_1 was prepared in two sequential steps, with the coupling of two known synthons, 4-(tert-butyldiphenylsilyloxy)benzyl chloride and 7-hydroxy-8-formylcoumarin, through a simple S_N2 reaction to yield 7-((4-(tert-butyldiphenylsilyloxy)benzyl)oxy)-8-formylcoumarin (DPA_1) [29, 33]. Fluorides were transferred to DPA_1 by treatment with (diethylamino)sulfur trifluoride (DAST), yielding DPF_1 (Scheme S1). Interestingly, fluoride transfer was successful in the presence of 4-tert-butyldiphenylsilyl functionality at low temperature, without interference from the special chemical affinity between fluoride and silicon, which would have resulted in the self-immolative disassembly of DPF_1. The overall yield of the two steps was 16%. The chemical structures of the synthetic intermediates and the final products were determined by ^{1}H and ^{13}C NMR and by mass spectrometry (Supporting Information).

3.1. Fluoride detection at DPF_1

The sensing ability of the DPF_1 was determined by recording its fluorescence spectra (λ_{ex} = 360 nm, λ_{em} = 445 nm) at different fluoride concentrations. In each analysis, DPF_1 was incubated in an APW solution for 1 h at 60ºC (Figure 1a). In the absence of fluoride, the optical switch, DPF_1 produced little fluorescence (Figure 1a). Introduction of 0.5 pM fluoride, however, resulted in highly enhanced fluorescence, corresponding to the emission spectrum of free coumarin (b) [33]. Fluorescence intensity was increased as the fluoride concentration increased from 0.5 pM to 50 μM (Figure 1a). A plot between logarithms of fluorescence intensity versus logarithm of fluoride concentration is exhibited a linear relationship in a wide linear concentration range from 0.5 pM and 50 μM (Figure 1b). The LOD of this probe was sufficiently sensitive to detect the EPA mandated upper limit of fluoride concentration (2 ppm or 106 μM) in drinking water.

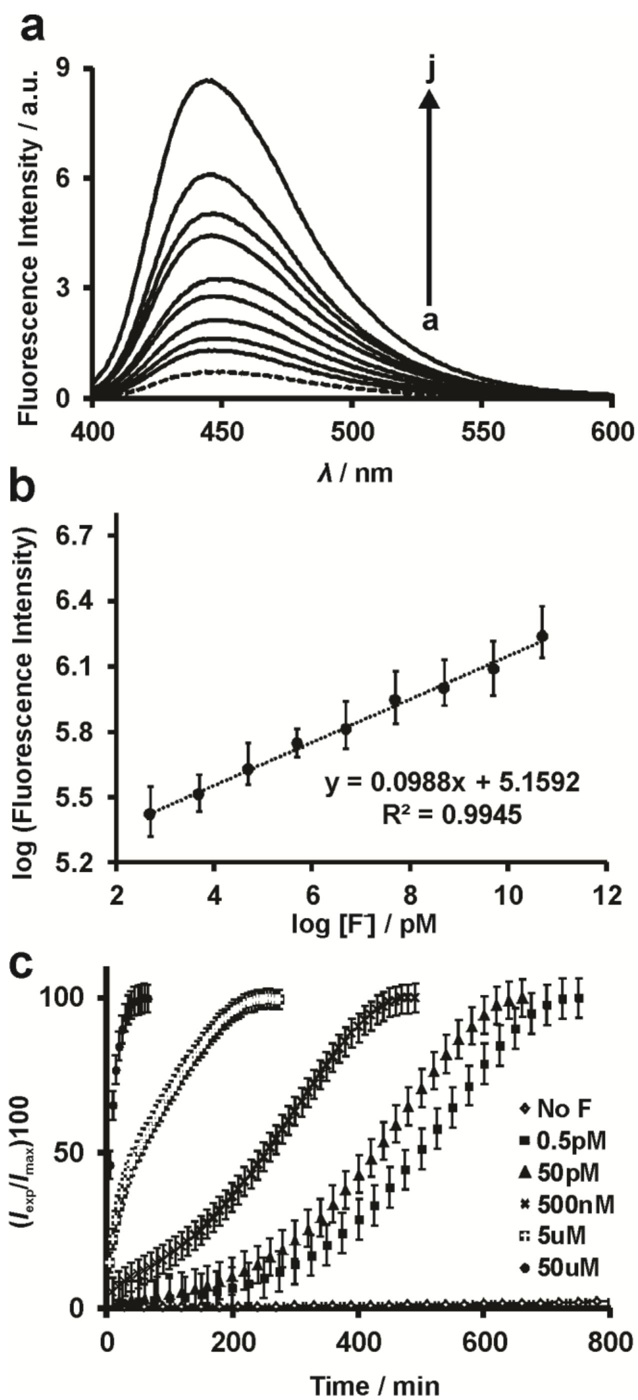

Fig. 1. (a) Fluorescence emission changes (λ_{ex} = 360 nm) of DPF_1 (50 µM) upon incubation with fluoride (a= 0, b= 0.5, c= 5, d= 5×10^1, e=5×10^2, f= 5×10^3, g= 5×10^4, h= 5×10^5, i= 5×10^6 and j= 5×10^7 pM) in APW solution for 1 h at 60ºC. (b) A log–log calibration curve of the reaction of DPF_1 with fluoride. (c) Kinetic analysis of fluorescence emission following the reaction of DPF_1

(50 μM) with 0 to 50 μM fluoride in APW solution at 40ºC via auto-inductive signal amplification.

3.2. Kinetic analysis for the fluoride detection at DPF_1

Kinetic analysis showed that the reaction of the fluoride with DPF_1 (50 μM) in APW solution at 40ºC was characteristic of an exponential progress of disassembly (Figure 1c). The relationship between percent fluorescence intensity ($[I_{exp}/I_{max}] \times 100$) of the released reporter b and time is expressed as a sigmoidal curve for each concentration of fluoride which confirmed the exponential amplification of the signal expected for an autoinductive process [7, 35]. Here, I_{exp} is fluorescence signal obtained at a particular time for each concentration of fluoride, while I_{max} is the maximum fluorescence signal following complete exposure to DPF_1. In the presence of 0.5 pM fluoride, reporter b begins to liberate from DPF_1 within 30 min and reached a maximum fluorescence signal at 700 min which indicating the complete disassembly DPF_1 at 700 min. In the absence of fluoride, however, DPF_1 does not emit fluorescence (Fig. 1c). This was not due to the instability of DPF_1, since the latter remained stable even after incubation for 35 h (data not shown). In the presence of low concentrations of fluoride, the probe requires long time for the complete disassemble. Thus, maximum autoinductive amplification process shows slower kinetics at lower concentrations.

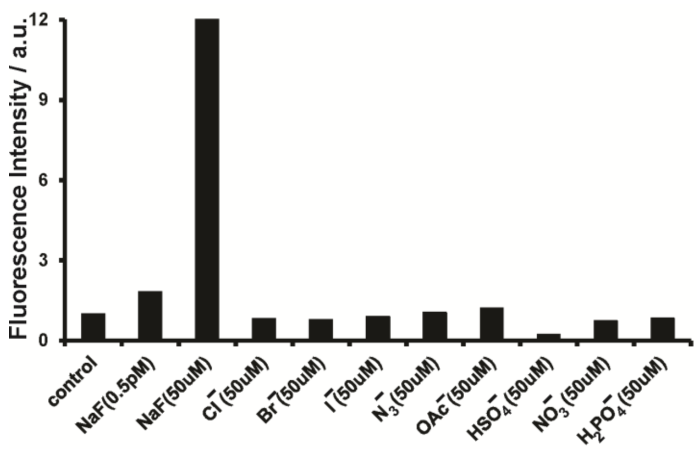

Fig. 2. Fluorescence emissions of DPF_1 upon incubation with fluoride (0.5 pM, 50 μM) and other anions (1 equivalent) in APW solution for 1 h at 60ºC. The control sample refers to the absence of any anions.

3.3. Selectivity

The selectivity of DPF_1 to the fluoride ions was investigated by testing several other common anions, including Cl^-, Br^-, I^-, N_3^-, CH_3COO^-, HSO_4^-, NO_3^- and $H_2PO_4^-$. Of these ions, only fluoride elicited a strong fluorescence signal from DPF_1, whereas all the other anions are unable to produce significant signals above background (Fig. 2). These results revealing that the proposed system is highly specific for fluoride over other anions. Moreover, our results are similar to those of other fluoride probes, which utilize specific fluoride-induced silyl deprotection to uncloak masked fluorogenic probes [24-28].

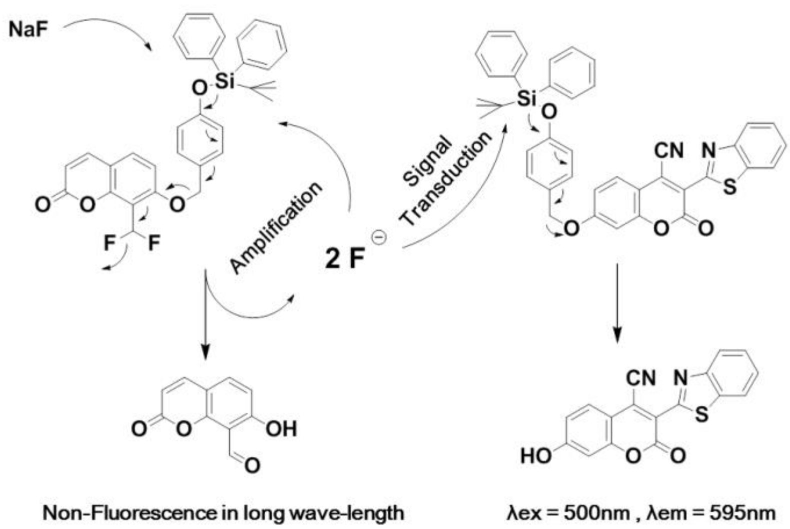

Scheme 2. A long wave fluorogenic probe (DCC) that uses an auto-inductive fluoride signal amplifier (DPF_1) to detect fluoride.

3.4. The role of autoinductive signal amplification

To investigate the role of autoinductive signal amplification mechanism embedded within DPF_1 aiming to improve its LOD, we prepared an analogous DPF_1 lacking the ability to undergo the autoinductive amplification reaction by substituting the geminal difluoride coumarin with the long fluorogenic molecule, 3-(2'-benzothiazolyl)-4-carbonitrile-7-hydroxycoumarin (DCC) (Scheme 2). The fluoride-induced signal revealing mechanism of DCC is same as that of DPF_1. DCC was revealed the fluorescence signals after incubation at 60°C for 5 h. However, LOD of this system to detect fluoride was found to be 238 nM, consistent with other fluoride detecting latent fluorescent probes (i.e. a LOD in the upper nanomolar range) [25]. Interestingly, LOD of DPF_1 towards fluoride detection was at least 10^5 fold more sensitive than DCC which revealing the crucial role of autoinductive amplification mechanism in improving the LOD from nanomolar to picomolar concentration. Therefore, incorporating autoinductive signal amplification into the design of an analyte detecting platform can boost the sensitivity of the assay system for determining very low concentrations of analyte.

3.5. The role of geminal fluorides as signal transduction agents

We also sought to demonstrate that the two geminal fluorides in DPF_1 released after the initiation of the self-immolative reaction are effective signal transduction agents. Co incubation of DPF_1 with DCC in the presence of fluoride should unlock coumarin, the moiety with long wavelength fluorescence in DCC (scheme 2). The fluorescence spectrum of the signal transduction system for DPF_1 (50 μM) coupled with DCC (5 μM) was tested by the addition of fluoride in APW solution; we deliberately designed this assay platform so that DPF_1 was present at a 10-fold higher concentration than DCC. Therefore, the initial fluoride would more likely interact with DPF_1 rather than with DCC. Figure 3 (a) presents the fluorescence spectra of the two probe system (5 μM DCC and 50 μM DPF_1) in the presence and absence of fluoride at different λ_{ex} and λ_{em}. As shown in Figure 3a (left), the fluorescence spectrum (λ_{ex} = 360 nm, λ_{em} = 445 nm) was characterized by the strong fluorescence signal of coumarin (b) released from DPF_1 in the presence of fluoride (50 pM) after incubation for 1 h at 60ºC. These findings suggested that the geminal fluorides in DPF_1 were released into the medium as two free fluoride ions. Upon approaching DCC, these fluorides could induce the removal of silyl ether protecting groups, which initiating a cascade of self-immolative reactions to eject long-wavelength coumarin (c) (λ_{ex} = 500 nm, λ_{em} = 595 nm) (Figure 3a, right).

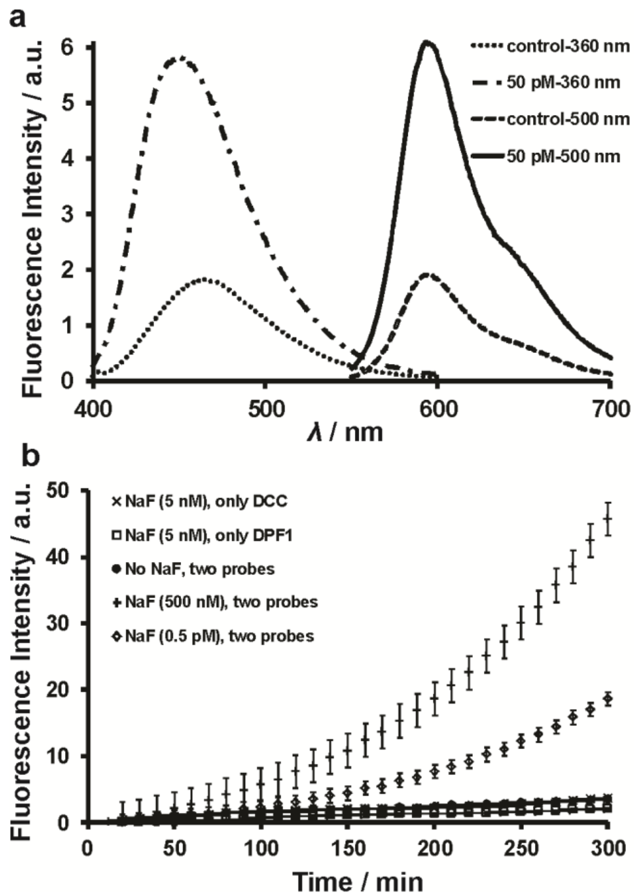

Fig. 3. Changes in fluorescence emission through λ_{ex} = 360 nm (left) and λ_{ex} = 500 nm (right) of two probes, DCC (5 µM) and DPF_1 (50 µM), in the presence of fluoride (50 pM) at 1 h (left) and 2 h (right) in APW solution at 60ºC. (b) Kinetic analysis of fluorescence emissions (λ_{ex} = 500 nm) of DPF_1 (50 µM), DCC (5 µM), and a two probe system, consisting of DCC (5 µM) and DPF_1 (50 µM), in the presence of low concentration of fluoride (0.5 pM and 500 nM) in APW solution at 40ºC.

3.6. Fluoride detection using two probes approach (DPF_1 and DCC)

Kinetic analysis indicated that neither DPF_1 nor DCC alone was able to emit fluorescence (λ_{ex} 500 nm) in the presence of a low concentration (0.5 pM) of fluoride, even after incubation for 300 min (Fig. 3b). In contrast, incubation of both probes in APW solution at 40°C with 0.5 pM and 50 pM fluoride increased the fluorescence emission spectra within 50 and 90 min, respectively (Fig. 3b). Only when the concentration of DPF_1 exceeded that of DCC, we were able to detect these low concentrations of fluoride with two probe coupling assay method.

Furthermore, LOD of DCC for the fluoride detection was 238 nM, but the LOD was 10^5 fold lowered when DCC is coupled DPF_1 which indicating the outstanding sensitivity of these two probes method. These results are revealing that the 2 geminal fluorides in DPF_1 available after activation are effective signal transduction agents that can remove other silyl ether trigger probes.

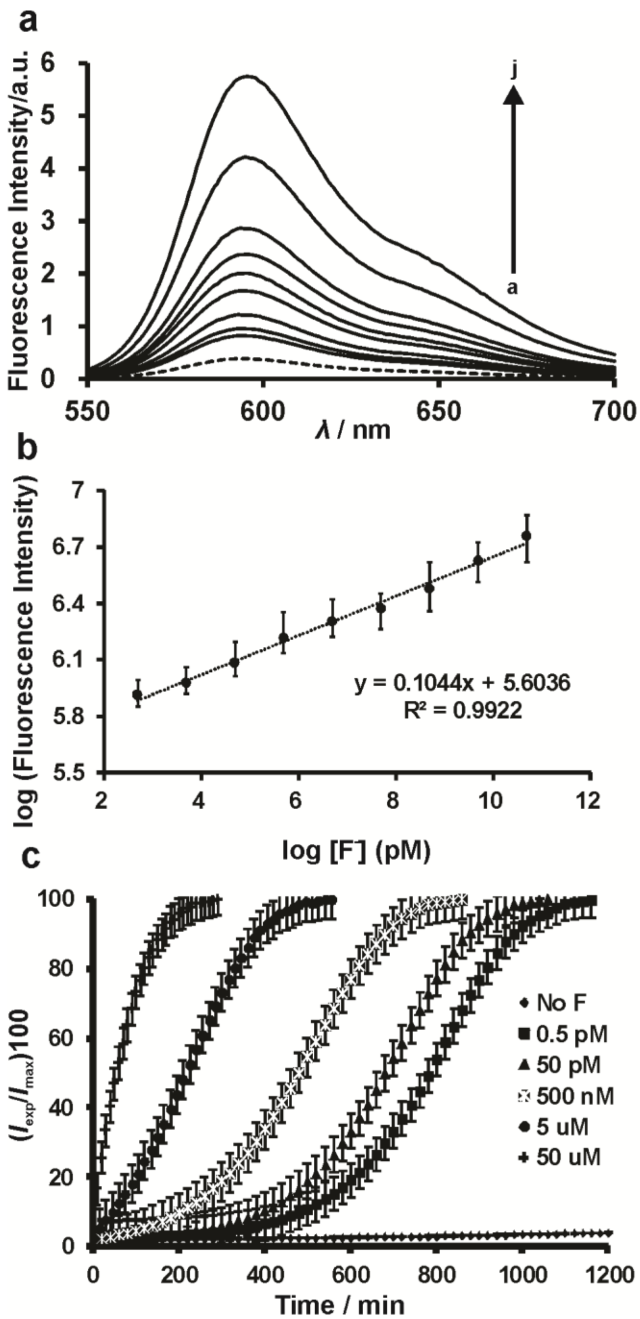

Fig. 4. (a) Fluorescence emission changes (λ_{ex} = 500 nm) of a two probe system, consisting of DCC (5 μM) and DPF_1 (50 μM), in the presence of various concentrations of fluoride (a= 0, b= 0.5, c= 5, d= 5×10^1, e=5×10^2, f= 5×10^3, g= 5×10^4, h= 5×10^5, i= 5×10^6 and j= 5×10^7 pM) in APW solution after 2 h at 60ºC. (b) Log–log calibration curve of the reaction of the two probe system, as above, with various concentrations of fluoride. (c) Kinetic analysis of fluorescence emission following the reaction of the two probe system with various concentration of fluoride in APW solution at 40ºC.

Fluorescence emission spectra (λ_{ex} = 500 nm) of the two probe system [DCC (5 μM) and DPF_1 (50 μM)] were recorded in the presence of various concentrations of fluoride following incubation in APW solution for 2 h at 60ºC (Figure 4a). Fluorescence increased with fluoride concentration (Figure 4a). A plot between logarithms of fluorescence intensity versus logarithm of fluoride is exhibited a linear relationship over a wide concentration range, from 0.5 pM to 50 μM (Figure 4b). Kinetic analysis of the two probe system [DCC (5 μM), DPF_1 (50 μM)] in the presence of various concentrations of fluoride is showed an exponential progression of disassembly, similar to that of DPF_1 (Figure 4c). Notably, comparing Figures 1c and 4c, a delay is observed in the disassembly of DCC in the two probe coupling assay, whereas rapid signal unmasking was observed for DPF_1. The time required for complete disassembly of DCC in the two probe system was nearly twice that of DPF_1 at the same fluoride concentration, with the delay in the former is likely due to the concentration differences in DPF_1 and DCC. The initially ejected latent fluorides from DPF_1 would be more likely to react with unreacted DPF_1 than with DCC due to the 10-fold difference in their concentrations. As the reaction progresses, most of the unreacted DPF_1 becomes depleted which resulting in the increase of free fluoride ions. These ions can catalyze the self-immolative reaction of DCC, unmasking long wavelength fluorogenic molecules

3.7. Advantages of the proposed approach over other methods

The LOD of our DPF_1 fluoride assay platform was much better than the LODs of existing methods of fluoride detection [21-29]. In addition, the synthesis of DPF_1 is easy and straightforward. Moreover, we are able to extend this fluoride detection platform to incorporate a long wavelength fluorescence probe, DCC. Many biological samples show some fluorescence of their own, typically in the blue region of the spectrum. Since this would interfere with the measurement of fluoride fluorescence, it is desirable to enhance the sensitivity of the detection by using marker dyes that fluoresce in a low-energy region (≥ 600 nm) of the electromagnetic spectrum [36]. Our two probe coupled amplification strategy is resulted in a long wavelength reporter with sensitivity in the sub-picomolar range with a detection time as short as 2.5 h. Our findings indicate that this method will constitute a novel and advanced platform for the fluoride analysis in biological samples.

Table 1 Determination of fluoride present in various water and urine samples using two probes approach (DPF_1 and DCC)

Samples	Added	Found	Recovery/%	*RSD/%
Tap water	5 nM	4.81 nM	96.2	2.83
	5 µM	4.85 µM	97.0	3.57
Rain water	5 nM	4.80 nM	96.0	2.33
	5 µM	4.91 µM	98.2	3.28
Pond water	5 nM	4.79 nM	95.8	2.80
	5 µM	4.90 µM	98.0	2.88
Urine sample	5 nM	4.92 nM	98.4	2.25
	5 µM	4.90 µM	98.0	2.47

* Relative Standard Deviation of 3 individual measurements.

3.8 Real sample analysis and repeatability studies

We have demonstrated the real sample analysis of the proposed sensor (two probes approach) towards determination of fluoride present in human urine sample and water samples (tap, rain and pond). The urine sample was collected from a healthy man and filtered a with whatman filter paper and diluted to the ratio of 1: 50 with the addition of APW solution. The spiked fluoride concentrations are 5 nM and 5 µM. The found and recovery values are given in Table 1. The acceptable recoveries obtained for the water and urine samples revealing the promising practical feasibilty of the sensor. Moreover, the sensor has offered appreciable repeatability towards determination of 5 nM fluoride with an R.S.D of 3.36% for five repeated measurements.

4. Conclusions

In summary, we have successfully implemented a quinone-methide-type rearrangement reaction as an off–on fluorometric switch and incorporated the concept of signal amplification into the design to prepare an ultrasensitive latent fluorogenic probe, DPF_1, for the sensitive detection of fluoride. DPF_1 in the presence of fluoride undergoes a cascade of self-immolative reactions with concomitant ejection of fluorogenic coumarin and two additional fluorides, leading to a continuous signal revealing process to achieve signal amplification with high sensitivity. The LOD of this probe surpasses the LODs of existing methods for fluoride detection. The fluorescence signal generated by this tandem reaction is highly specific and insensitive to other anions. Furthermore, DPF_1 coupled with the long wavelength DCC probe can act as a sensitive fluorometric indicator to quantitatively measure fluoride in long wavelength spectra, thus avoiding any interference by biological samples. The practical applicability of the proposed approach has been demonstrated in water samples with appreciable recoveries. The assay platform coupling DPF_1 and DCC should be applicable to measure fluoride in biological samples. In future, this assay system may be used to construct fiber-optic sensors.

Acknowledgment

This work was supported by the Ministry of Science and Technology, Taiwan (NSC 103-2811-M-027-002 and 102-2113-M-027-002-MY3).

References

1. D. A. Giljohann and C. A. Mirkin, *Nature*, 2009, 462, 461-464.
2. J. P. Gosling, *Clinical Chemistry*, 1990, 36, 1408-1427.
3. S. GreenER, *Nature Methods*, 2007, 4, 869.
4. J.-M. Nam, C. S. Thaxton and C. A. Mirkin, *Science*, 2003, 301, 1884-1886.
5. P. Scrimin and L. J. Prins, *Chemical Society Reviews*, 2011, 40, 4488-4505.
6. N. Karton-Lifshin and D. Shabat, *New Journal of Chemistry*, 2012, 36, 386-393.

354 7. M. S. Baker and S. T. Phillips, *Journal of the American Chemical Society*, 2011, 133, 5170-5173.
356 8. E. Sella, A. Lubelski, J. Klafter and D. Shabat, *Journal of the American Chemical Society*, 2010, 132, 3945-3952.
358 9. E. Sella, R. Weinstain, R. Erez, N. Z. Burns, P. S. Baran and D. Shabat, *Chem. Commun.*, 2010, 46, 6575-6577.
360 10. M. Avital-Shmilovici and D. Shabat, *Bioorganic & medicinal chemistry*, 2010, 18, 3643-3647.
362 11. E. Sella and D. Shabat, *Journal of the American Chemical Society*, 2009, 131, 9934-9936.
364 12. L. Zhu and E. V. Anslyn, *Angewandte Chemie International Edition*, 2006, 45, 1190-1196.
366 13. M. S. Baker and S. T. Phillips, *Organic & biomolecular chemistry*, 2012, 10, 3595-3599.
367 14. Y. Wu, X. Peng, J. Fan, S. Gao, M. Tian, J. Zhao and S. Sun, *The Journal of organic chemistry*, 2007, 72, 62-70.
369 15. H. Matsui, M. Morimoto, K. Horimoto and Y. Nishimura, *Toxicology In Vitro*, 2007, 21, 1113-1120.
371 16. P. Singh, M. Barjatiya, S. Dhing, R. Bhatnagar, S. Kothari and V. Dhar, *Urological research*, 2001, 29, 238-244.
373 17. M.-L. Cittanova, B. Lelongt, M.-C. Verpont, M. Geniteau-Legendre, F. Wahbe, D. Prie, P. Coriat and P. M. Ronco, *Anesthesiology*, 1996, 84, 428-435.
375 18. U. EPA, *Total Coliforms (Including Fecal Coliforms and E. Coli)*, 2009, 54.
376 19. Y. Zhou, J. F. Zhang and J. Yoon, *Chemical reviews*, 2014.
377 20. R. Martínez-Máñez and F. Sancenón, *Chemical reviews*, 2003, 103, 4419-4476.
378 21. S. Rivadehi, E. F. Reid, C. F. Hogan, S. V. Bhosale and S. J. Langford, *Organic & biomolecular chemistry*, 2012, 10, 705-709.
380 22. Y. Qu, J. Hua and H. Tian, *Organic letters*, 2010, 12, 3320-3323.
381 23. M. Cametti and K. Rissanen, *Chemical Communications*, 2009, 2809-2829.
382 24. J. Du, M. Hu, J. Fan and X. Peng, *Chemical Society Reviews*, 2012, 41, 4511-4535.
383 25. S. Y. Kim and J.-I. Hong, *Organic letters*, 2007, 9, 3109-3112.

26. S. Elsayed, A. Agostini, L. E. Santos-Figueroa, R. Martínez-Máñez and F. Sancenón, *ChemistryOpen*, 2013, 2, 58-62.
27. R. Hu, J. Feng, D. Hu, S. Wang, S. Li, Y. Li and G. Yang, *Angewandte Chemie International Edition*, 2010, 49, 4915-4918.
28. S. Y. Kim, J. Park, M. Koh, S. B. Park and J.-I. Hong, *Chemical Communications*, 2009, 4735-4737.
29. J.-A. Gu, Y.-J. Lin, Y.-M. Chia, H.-Y. Lin and S.-T. Huang, *Microchimica Acta*, 2013, 180, 801-806.
30. H.-C. Huang, K.-L. Wang, S.-T. Huang, H.-Y. Lin and C.-M. Lin, *Biosensors and Bioelectronics*, 2011, 26, 3511-3516.
31. S.-T. Huang, C.-J. Teng, Y.-H. Lee, J.-Y. Wu, K.-L. Wang and C.-M. Lin, *Analytical chemistry*, 2010, 82, 7329-7334.
32. S.-T. Huang, K.-N. Ting and K.-L. Wang, *Analytica chimica acta*, 2008, 620, 120-126.
33. D. H. Kwan, H. M. Chen, K. Ratananikom, S. M. Hancock, Y. Watanabe, P. T. Kongsaeree, A. L. Samuels and S. G. Withers, *Angewandte Chemie*, 2011, 123, 314-317.
34. R. Perry-Feigenbaum, E. Sella and D. Shabat, *Chemistry-A European Journal*, 2011, 17, 12123-12128.
35. M. H. Todd, *Chemical Society Reviews*, 2002, 31, 211-222.
36. A. Gómez-Hens and M. Aguilar-Caballos, *TrAC Trends in Analytical Chemistry*, 2004, 23, 127-136.